QUATERNARY RESEARCH 27, 1–29 (1987)

Age Dating and the Orbital Theory of the Ice Ages: Development of a High-Resolution 0 to 300,000-Year Chronostratigraphy[1]

DOUGLAS G. MARTINSON,* NICKLAS G. PISIAS,† JAMES D. HAYS,* JOHN IMBRIE,‡ THEODORE C. MOORE, JR.,§ AND NICHOLAS J. SHACKLETON‖

Lamont-Doherty Geological Observatory, Palisades, New York 10964, and Department of Geological Sciences, Columbia University, New York, New York 10027; †College of Oceanography, Oregon State University, Corvallis, Oregon 97331; ‡Department of Geological Sciences, Brown University, Providence, Rhode Island 02912; §Exxon Production Research, Houston, Texas 77001; and ‖Sub-Department of Quaternary Research, The Godwin Laboratory, Free School Lane, Cambridge, England CB2 3RS

Using the concept of "orbital tuning," a continuous, high-resolution deep-sea chronostratigraphy has been developed spanning the last 300,000 yr. The chronology is developed using a stacked oxygen-isotope stratigraphy and four different orbital tuning approaches, each of which is based upon a different assumption concerning the response of the orbital signal recorded in the data. Each approach yields a separate chronology. The error measured by the standard deviation about the average of these four results (which represents the "best" chronology) has an average magnitude of only 2500 yr. This small value indicates that the chronology produced is insensitive to the specific orbital tuning technique used. Excellent convergence between chronologies developed using each of five different paleoclimatological indicators (from a single core) is also obtained. The resultant chronology is also insensitive to the specific indicator used. The error associated with each tuning approach is estimated independently and propagated through to the average result. The resulting error estimate is independent of that associated with the degree of convergence and has an average magnitude of 3500 yr, in excellent agreement with the 2500-yr estimate. Transfer of the final chronology to the stacked record leads to an estimated error of ±1500 yr. Thus the final chronology has an average error of ±5000 yr.

INTRODUCTION

Numerous investigators have shown that the earth's climate responds linearly, to some unresolved extent, to variations in the earth's orbital geometry (e.g., Hays *et al.*, 1976; Kominz and Pisias, 1979). Since this climate response is continuously recorded in deep-sea sediments by climatically sensitive parameters, the orbital/climate link provides a unique opportunity for establishing a late Pleistocene geochronology. This can be achieved by considering the known history of the orbital forcing as an orbital "metronome," and the related portion (the climate response) embedded in the geological data, as a "metronomic record" (Fig. 1). The metronomic record is distorted while being recorded in deep-sea sediments by such things as changes in sedimentation rate. Provided the lag between the orbital forcing and climatic response is constant, tuning the climatic response to keep pace with the orbital metronome will yield an absolute chronology.

In this paper we use such an "orbital tuning" concept, first developed by Milankovitch (1941), to create a continuous, high-resolution chronostratigraphy based upon a high-resolution, well-controlled oxygen-isotope stratigraphy (Pisias *et al.*, 1984). We also assess the overall sensitivity of an orbitally based chronology to various assumptions associated with orbital tuning techniques and attempt to estimate the error envelope associated with the resultant chronology. Our strategy involves the use of four different orbital tuning approaches. Obviously, these approaches are not independent, as they all depend on the specific assumption of orbital forcing.

[1] LDGO Contribution Number 3994.

0033-5894/87 $3.00

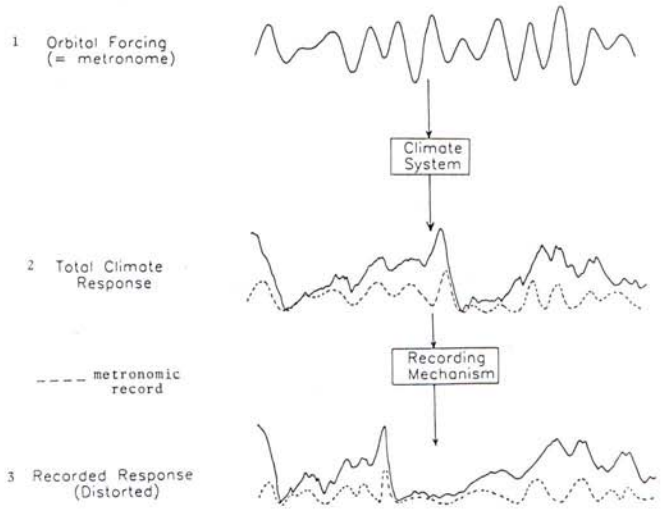

FIG. 1. Schematic representation of the three levels involved in the recording of the climate record. Level numbers are referred to in Table 1.

Each, however, does make a different assumption as to the exact nature of the metronomic record and how it should be manipulated and tuned (Table 1). Consequently, each approach is susceptible and more sensitive to different errors. Since some of the approaches utilize more than one climatic indicator, biases associated with any one particular recording of the climate are eliminated.

Each of our four orbital tuning approaches produces a unique chronology. The differences between these chronologies reveal the sensitivities of the specific tuning techniques and their underlying assumptions. They also provide a basis from which to select and evaluate the reliability of a "best" time scale. Furthermore, their degree of convergence helps answer questions related to the orbital/climate link. In this way we (1) obtain the highest resolution orbitally based geochronology, (2) estimate its limitations, and (3) obtain information about the degree to which variations in the earth's orbit affect global climate. Furthermore, the results here can be used to assess the long, lower resolution orbitally based chronology of Imbrie *et al.* (1984) which was limited to a single climatic indicator ($\delta^{18}O$) and one tuning technique.

STRATIGRAPHY AND DATA

A geological time scale is only as useful as the stratigraphic framework on which it is built. That is, stratigraphic knowledge permits the identification and elimination of disturbances in individual records and stratigraphic correlation makes it possible to apply a given time scale universally. Pisias *et al.* (1984) correlated and stacked seven globally representative benthic-foraminiferal-based oxygen-isotope records to construct a "standard" stratigraphy for deep-sea sediments spanning about the last 300,000 yr. The stacking serves to enhance the signal-to-noise ratio and eliminate flaws present in individual records. Over 40 well-defined features survived this stacking process, suggesting that high-frequency variations in the global climate system are recorded and preserved with remarkable fidelity in the marine sediment record. Their results indicate that detailed correlations are possible at the sampling interval (2000–4000 yr in the records used). The Pisias *et al.* (1984) stratigraphy therefore

provides an excellent framework upon which a high-resolution deep-sea chronology can be built.

Any core with sufficient stratigraphic quality and temporal resolution can be tied into the Pisias *et al.* (1984) stratigraphic framework. We develop our chronology in core RC11-120, from the southwestern subpolar Indian Ocean. This core was chosen from several hundred examined for the Hays *et al.* (1976) testing of the orbital theory of climatic forcing. It has the necessary quality and temporal resolution, and offers several distinct advantages as well.

Most importantly, RC11-120 provides five climatically sensitive data sets (Fig. 2; values in Appendix): planktonic, and limited benthic (upper ~3 m), oxygen-isotope measurements ($\delta^{18}O$); relative abundance of the radiolarian *Cycladophora davisiana;* estimates of summer sea surface temperature (TS); carbon isotope measurements ($\delta^{13}C$); and percentage $CaCO_3$ present. Measurements of the first three parameters were made at 10-cm intervals and presented in Hays *et al.,* 1976. This sampling interval has since been increased to 5 cm for all parameters except percentage $CaCO_3$ which is presented at 20-cm intervals.

The exact climatic significance of these parameters, or "paleoclimatic indicators," is uncertain (Shackleton 1977; Broecker, 1982; Shackleton and Opdyke, 1973; Hays *et al.,* 1976; Imbrie and Kipp, 1971; Berger, 1973; Dunn, 1982; Moore *et al.,* 1982). Regardless, despite differences in the character of the individual records, they all display some similarities in the timing of certain peaks and troughs (Fig. 2). These parameters should therefore provide a good basis on which to test or improve several of the tuning approaches and to free the results from bias associated with any one particular recording of the climate signal.

In addition to the above, the availability of both benthic and planktonic oxygen-isotope data aids in evaluating errors introduced by transferring the chronology to the benthonic-based stratigraphic framework. The core has a time scale, established independently of orbital tuning techniques (Hays *et al.,* 1976), providing initial time control to minimize problems associated with filtering the data, as required in the first approach. Also for that approach, the $\delta^{18}O$ record can be extended by almost 200,000 yr by appending an overlapping isotope record from core E49-18 (Hays *et al.,* 1976). This extension minimizes information loss due to the filtering process. Together, these unique advantages of RC11-120 make it ideal for developing a high-resolution chronology.

PHASE LOCKED APPROACH

Assumptions and Potential Error Sources

In this tuning approach we assume that the phase (i.e., lags) between the dominant components of the orbital forcing, obliquity, and precession, and the corresponding components recorded in the geological data, are constant over the last 300,000 yr. To implement this approach we must (1) determine what these lags are and (2) adjust the chronology to force these lags to be constant over the length of the record. This should provide a chronology accurate to the degree to which the assumption of constant phase is true and the accuracy with which the lags are determined and imposed.

The desired lag values and the precision at which they are determined are estimated from RC11-120 using the initial, independent chronology established for that core by Hays *et al.* (1976; their ELBOW time scale). Over that interval which has the most certain chronology, 0 to 150,000 yr, the precessional component extracted from the $\delta^{18}O$ record lags true precession by about 7600 $\pm$ 1700 yr. As described below, the error associated with this, the shortest period component, controls this error term.

TABLE 1. SUMMARY OF THE VARIOUS ORBITAL TUNING APPROACHES USED (NUMBERS REFERRED TO CORRESPOND TO THE THREE LEVELS OF FIGURE 1)

Tuning approach	Underlying assumption	Implementation procedures	Phase (response time) determination	Data set(s) used	Potential sources of error
Phase locked	Metronomic record in data (3) maintains constant phase relationship (over last 300 × 10^3) to corresponding orbital forcing components (1)	Isolate metronomic record from climate signal (3) by bandpass filtering; then force a phase locked relationship by correlating to metronome (1)	From "ELBOW" time scale of Hays *et al.*, 1976 (independent of orbital tuning techniques)	Initial tuning made using Ts and *C. davisiana* from RC11-120; final tuning using $\delta^{18}O$ of RC11-120	1. Quality of assumption 2. Ability to determine appropriate phase relationship 3. Success of isolating metronomic record, dependent upon a. Accuracy of initial chronology b. Proportion and distribution of nonmetronome (extraneous) variance in 3 c. Filter width vs width of smeared metronomic record frequency bands 4. Precision with which metronomic record (3) is correlated to metronome (1)
Direct response	Climate responds by mimicking orbital forcing, so 3 is simply a distorted version of 1 (and 2)	Correlate the climate signals (3) to the orbital forcing (= summer irradiation at 65°N; 1)	From minimum response parameter in RC11-120, assumed to represent instantaneous response	From RC11-120: *C. davisiana*, $\delta^{18}O$, $\delta^{13}C$, $CaCO_3$	1. Quality of assumption 2. Degree to which proper irradiation curve is identified 3. Accuracy at which climate response time is determined 4. Precision with which data is correlated to irradiation curve

Nonlinear response	Climate responds nonlinearly to forcing, so 2 is a nonlinear response to 1, and 3 is a distorted version of 2	Correlate the climate signal (3) to the climate response signal (2; predicted by Imbrie and Imbrie, 1980, model)	From nonlinear response model of Imbrie and Imbrie, 1980	$\delta^{18}O$ record of RC11-120	1. Quality of assumption 2. Degree to which proper climate response curve is determined 3. Accuracy at which climate response time is determined 4. Precision with which data are correlated to climate response curve
Pure components	Climate response signal (2) is dominated by major orbital components (precession and obliquity) and their harmonics	Combine pure orbital components and their harmonics (determined by spectral analysis of data, 3, with independent chronology) to create climate response curve (2) and correlate climate record (3) to it	Initial phase from ELBOW time scale of Hays *et al.*, 1976; final phase from small adjustments (within predicted errors bars) to produce signal with relative phasing most similar to overall data. Phase of harmonics set by that of precession and obliquity	Benthic $\delta^{18}O$ stacked record of Pisias *et al.*, 1984	1. Quality of assumption 2. Degree to which proper phase relationship between precession and obliquity is determined 3. Precision with which data is correlated to climate response curve 4. Transfer to RC11-120

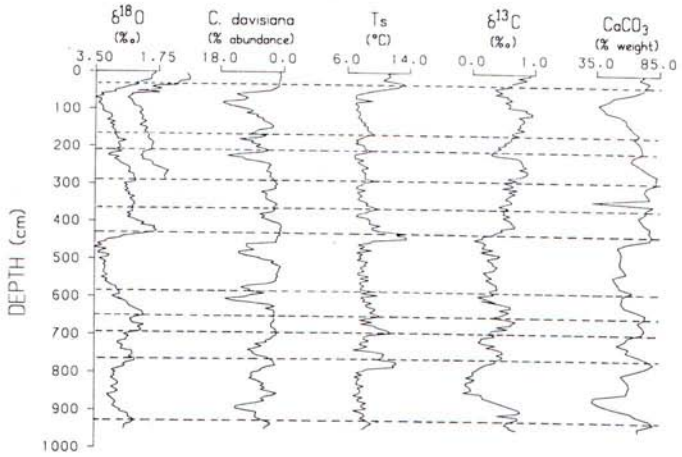

FIG. 2. Five climatically responsive parameters present in deep-sea sediment core RC11-120 (values given in Appendix). Presented at 5-cm intervals except for $CaCO_3$ which is at 20-cm intervals. Correlative lines show relationship between timing of the peaks in the various curves.

The error associated with the underlying assumption (that the above determined phase lag is constant) is estimated by computing the deviation from this 7600-yr lag over the entire length of the time series with the ELBOW chronology as the time base. This results in a systematic error of 1700 ± 2000 yr. This error should be added to that associated with the ELBOW chronology (±5%, at best), but we choose to bypass this radiometric error in favor of the orbital assumption. That is, instead of maintaining a dependence on absolute radiometric dating, we rely on the assumption that the orbital metronome is recorded to some degree in the data. This ±5% error is therefore ignored in all of the approaches, although its affect here is to limit the above error estimate to a "best" case, or underestimate.

The error associated with our ability to impose the constant phase lag accurately is determined upon completion of the tuning. Experience shows that the magnitude of this error will be small relative to those already discussed.

Finally, the orbital components (metronomic record) must be filtered from the data in order to impose the constant phase lags. This introduces a fourth source of error. If the initial age control is inaccurate when the filtering is done, extraneous signal variance (nonlinear orbital and non-orbital-related components) is shifted or smeared into the band being filtered, while some of the metronomic record is shifted or smeared out of the band. This degrades and distorts the extracted metronomic record, which in turn limits our ability to tune the climate signal. The degree of degradation is dependent upon the magnitude of the errors in the initial chronology, the nature of their distribution throughout the length of the record being filtered, the width of the filter, and the proportion and distribution of extraneous frequency components present in the climate signal. The magnitude of this error is estimated through a controlled sensitivity study, briefly summarized below.

Sensitivity Tests

The initial tests were designed to determine the optimal filter width for extracting the obliquity component from the climate record under the worst case conditions: a 5% error in an initial chronology, distributed over the 400,000-yr length of an artifi-

cial climate signal in a rapidly changing manner (from the full negative to full positive error in a time span of 50,000 yr). The tests involved filtering this distorted climate signal with filters of varying width, then tuning (phase locking) the extracted obliquity component with the true (undistorted) obliquity component. The optimal filter is the narrowest one capable of extracting enough obliquity signal to allow a successful tuning.

Test results indicate that the filter must be wide enough to include essentially all of the distorted obliquity component variance, including that which has been smeared to neighboring frequency bands. This width is so great that it captures significant power from the extraneous components in the general frequency range of the obliquity component and adulterates the extracted signal enough to make the tuning erroneous and misleading. This includes cases in which the tuned obliquity component displays a high coherence with true obliquity.

Furthermore, a narrower filter cannot be used to isolate some of the metronomic record (and none of the extraneous components) and partially eliminate the error allowing an iterative tuning approach. Therefore, the obliquity component, extracted by bandpass filtering techniques, is so sensitive to chronological error that it cannot be reliably used to tune the time scale. For errors less than the worst case, successful tuning is possible; however, in practice it cannot be assumed that the errors are less than the worst case.

Tests involving the precessional component were even less successful. With precession, though, its strong modulation due to the closeness of its dominant frequency components (periods 23,000 and 19,000 yr) has some advantages. Our tests suggest that while a high coherency between the tuned precessional component (in the data) and true precession does not uniquely indicate a correct tuned result, a successful match of the timing and relative amplitudes of the modulations (i.e., the envelopes) between these components does indicate that the correct tuned results has been obtained.[2] Thus, obliquity and precession can be successfully filtered for tuning purposes only when the initial error is small (magnitude $\leq 3\%$ and going from the full positive to full negative amount over time spans of about 100,000 yr). In any case, the success of the tuning can be tested by comparing the shape of the envelopes between the extracted components (from the tuned signal) and the corresponding orbital components. In fact, we find that the tuning can be successful to ± 2000 yr using just the extracted precessional component. This includes that error associated with our ability to impose the constant phase lag.

Implementation

In order to assure the best possible initial chronology, prior to filtering, we first tune using two of the climate records from RC11-120, each of which is dominated by a single orbital component. These include *C. davisiana* and Ts. As shown by Hays *et al.* (1976), *C. davisiana* is dominated by obliquity and Ts by precession. Therefore we treat these signals as if they *are* the extracted components by which they are dominated. This avoids the problem associated with filtering these components from the data as already discussed.

The phase lags to be imposed using the *C. davisiana* and Ts records are taken from Hays *et al.* (1976). Based on their ELBOW chronology, the obliquity component of *C.*

[2] This implies a relatively high coherency between the tuned and true components, but a high coherency does not guarantee that the modulation of the envelopes is in phase as required here. This is due to the fact that coherency measures this match integrated over the entire length of the signals. An isolated mismatch in envelope modulation does not necessarily degrade the coherency significantly. Therefore, while a high coherency is necessary to establish that a direct relationship exists between the components being compared, a match in the modulation of the envelopes is necessary to establish that the time base of the two components is the same.

davisiana lags true obliquity by ~7000 yr and the 23,000 yr precessional component of Ts lags the true component by ~3000 yr over the youngest 150,000 yr of the record. The time scale is adjusted to maintain these lags throughout the record length.

The modified time scale resulting from these adjustments is now used as the initial chronology for the $\delta^{18}O$ signal from which the precessional component is extracted for the final tuning stage. This record is filtered using a filter (gaussian, centered at 21,000 yr) determined in the previously described sensitivity study. Making the appropriate (further) adjustments to the time scale, the extracted precessional component is locked with a 7600-yr phase lag with true precession.

A final assessment of the success of this tuning is made by comparing the precessional component, extracted using this tuned time base, to true precession (Fig. 3). The timing and relative amplitudes of the two signals agree extremely well, which, as discussed previously, suggests a successful tuning. The chronology resulting from this approach is presented in Figure 4. The −5500- to +7500-yr error bars shown (rounded to the nearest 500 yr), result from linearly combining the −2000- to +3700-yr error associated with the quality of the underlying assumption (that the phase is constant), the ±1700-yr uncertainty in the phase determination, and the ±2000-yr error related to our ability to impose the constant phase lag accurately.

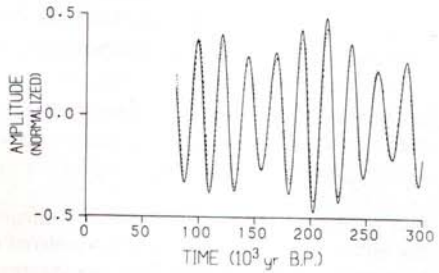

FIG. 3. Comparison of true precession (solid) and precessional component extracted from the phase-locked $\delta^{18}O$ record (dashed). Within resolution of the filtering operation, the two curves display a nearly perfect match in both shape and timing of their envelopes (arbitrary scale for the ordinate).

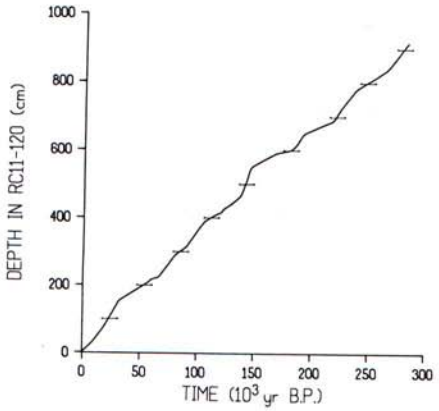

FIG. 4. Chronology resulting from the phase locked tuning approach. Error bars have a magnitude of −5500 to +7500 yr.

DIRECT RESPONSE APPROACH

Assumptions and Potential Error Sources

In this and the following approach we do not work solely with the metronomic record but with the complete unfiltered climate records. We must therefore assume knowledge of the nature of the climatic response to the orbital forcing. Here, the response is assumed to mimic simply the forcing, consistent with the original Milankovitch theory (1941) which suggests that the waxing and waning of continental ice sheets is in direct response to changes in solar irradiation at a particular latitude and time of year. Hence, the only difference between the recorded version of this response and the driving irradiation curve should be a distortion introduced by changes in the sediment accumulation rate which stretch and squeeze the recorded version relative to the forcing. This distortion is removed by correlating the data record to the forcing signal, or "tuning target." The accuracy of a chronology derived via this tuning technique is limited by the quality of the underlying assumption, the degree to which we correctly identify the proper irradiation

forcing curve and associated climate response time, and the precision with which the data are correlated to the tuning target.

The quality of the underlying assumption (that the response mimics the forcing) is certainly the dominant source of error. This error is dependent upon the amount and distribution of extraneous variance (noise) in the climate record, i.e., variance not attributable to a direct response to the forcing. Since the complete climate record is correlated to the forcing curve, this extraneous variance is forced to correspond to the tuning target regardless of what it is attributable to. This is "overtuning," which introduces noise into the age model or, worse, produces an erroneous chronology.

Fortunately, RC11-120 contains five different records of the climate response. Each is distinctly different in character (Fig. 2), as it represents a climatic indicator which responds in a different degree, or manner, to the forcing. Therefore, each contains a different (independent) distribution of extraneous variance or noise. If this noise is not overwhelming, individual chronologies resulting from correlating each record to the forcing should be grossly similar but differ in detail due to differences in the distribution of the noise. We then average these similar chronologies to minimize the noise and produce the best direct response chronology. The resulting statistics provide an estimate of the magnitude of the noise which is a direct measure of the quality of the underlying assumption. This is an underestimate, though, since the statistics do not account for any extraneous variance which manifests itself in a similar manner amongst the various climate records.

An upper limit for this error is made by considering the limiting case, expected if our underlying assumption were exactly correct. That is, as stated above, the effect of overtuning is to introduce noise (i.e., irregularities) into the true chronology. If no extraneous variance is present in the climate records, we might expect a chronology which is smooth relative to one containing irregularities (assuming, of course, that the irregularities are not consistently of equal magnitude and opposite sign to the sedimentation rate changes). An upper limit is thus obtained by determining the average magnitude of the irregularities about a smoothed version of the resulting chronology. We average this upper limit with the previous lower limit to produce a representative estimate of this potential source of error.

The magnitude of the error associated with the proper identification of the critical forcing irradiation curve is estimated from the literature. Milankovitch (1941) argued that the summer irradiation at 65°N is most crucial to the development or destruction of continental ice. The majority of recent workers (e.g., Broecker, 1966; Emiliani, 1966; Broecker *et al.*, 1968; Kominz and Pisias, 1979; Ruddiman and McIntyre, 1979; Imbrie and Imbrie, 1980) agree with Milankovitch that the high northern latitude during summer months is critical to the buildup or decay of glacier ice. Differences as to the exact latitude, however, vary from 45°N (Broecker, 1966; Broecker *et al.*, 1968) to 65°N (Milankovitch, 1941; Emiliani, 1966; Ruddiman and McIntyre, 1979; Imbrie and Imbrie, 1980) with 50°N (Kominz and Pisias, 1979) in between.

The major effect of latitude on the irradiation curve is to establish the relative amplitudes between the precession and obliquity components making up the irradiation curve. Over the range being considered here, the amplitude differences are fairly small and the effect on the timing of the irradiation peaks is essentially negligible. A correlation between the data and irradiation curve at any of these latitudes can therefore be expected to yield similar results.

Such is not the case for irradiation curves representing different times of the year. This timing controls the relative phasing of the two orbital components in

the irradiation curve and thus alters the timing of the peaks and valleys in the signal. Any discrepancies in this value will introduce uncertainties in the resulting chronology. While most workers agree that the summer months represent the critical time of year, the uncertainty is which summer month can introduce errors as large as ±1750 yr if the central month (July) is chosen (the absolute phase of the obliquity component is fixed, so the 360° of possible phase is equivalent to the precessional period, ~21,000 yr; thus a single month error introduces a phase error of ±1750 yr). This error is applicable to the $\delta^{18}O$ record. The response of the other climatic indicators may or may not be related to the disposition of continental ice sheets. However, Martinson (1982), studying the effects of phase errors on the resulting chronology itself, concludes that except for Ts, the July irradiation curve is most representative of the other data records (to within approximately one month). The Ts record is therefore not used in this approach.

While the four remaining climatic indicators, or parameters, of RC11-120 may all be responding in some manner to the same irradiation curve, they may have different response times. Since a parameter cannot respond before it has been forced, the parameter which leads all others (i.e., the one which produces the youngest age estimate at any particular depth) is the one whose chronology is closest in recovering the absolute chronology. If this "minimum response" parameter responds instantaneously to the forcing, then its chronology has no systematic offset from the absolute chronology.

We assume that the minimum response parameter *does* represent an instantaneous response. Thus, the error associated with not knowing the lag between the forcing and response of this parameter is systematic and given by the difference between an instantaneous response (the quickest a parameter can obviously respond) and the actual lag of the minimum response parameter. We must therefore estimate the true lag to determine the magnitude of this error. Since we estimate a chronology for each of the RC11-120 climatic indicators we obtain the relative lags between the various parameters. We also use a model (in the next approach) which predicts the absolute lag of $\delta^{18}O$ to be ~5000 yr. By combining the relative lag between the minimum response parameter and $\delta^{18}O$ with the predicted absolute lag of $\delta^{18}O$, we obtain an estimate of the absolute lag of the minimum response parameter. This provides an estimate of the error introduced by assuming an instantaneous time for the minimum response parameter.

Finally, to estimate a chronology from each climatic indicator of RC11-120, the records are correlated to the irradiation curve using the correlation method of Martinson *et al.* (1982). This method offers the advantage of quickly producing an objective and high-resolution, continuous correlation. The correlation is expressed by a "mapping function" which relates depth in the core to time in the irradiation curve and is thus the age model. The error introduced via this tuning is small relative to the other sources of error and easily assessed upon examination of the correlated results.

Implementation

The results of correlating the data records to the 65°N, July irradiation curve are shown in Figures 5a and b. The correlations are quite good despite a couple of obvious miscorrelations resulting from the large, relative-amplitude discrepancies between the data and tuning target which coincide with an apparent hiatus in the data (Martinson, 1982, p. 139). Smaller miscorrelations result from the difference in character between the data and irradiation curve. In all, these introduce errors of average magnitude <1000 yr which manifest themselves as slight irregularities in the chronology. Their effect is thus included in

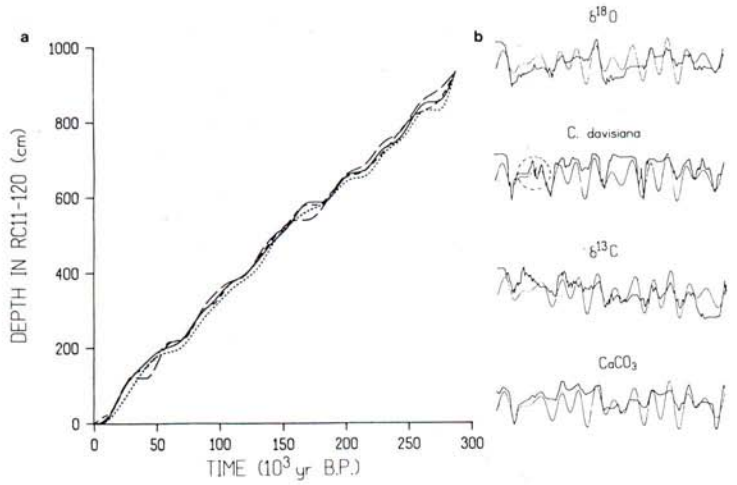

FIG. 5. (a) Age models for each parameter curve resulting from the direct response tuning approach ($\delta^{18}O$: solid; *C. davisiana:* long dash; $\delta^{13}C$: dotted; $CaCO_3$: short dash). (b) Correlations between each parameter curve (bold) and the 65°N, July irradiation curve (light). Dashed circle indicates areas of obvious miscorrelation.

the error estimate determined from the magnitude of the irregularities themselves.

Overall, the resulting chronologies look quite similar suggesting that the tuning technique is fairly insensitive to the particular recording of the climate signal. It also indicates that the extraneous variance is not overwhelming in the four records, so their chronologies can be averaged together after normalizing to the minimum response parameter, to produce the direct response chronology.

Examination of the results in Figure 5a reveals that *C. davisiana* is the minimum response parameter. Comparison of this result to the remaining ones indicates that it leads the $\delta^{18}O$ and $CaCO_3$ by ~2500 yr and $\delta^{13}C$ by ~7500 yr. Upon removal of these lags (Fig. 6) the superimposed chronologies are remarkably similar. Miscorrelations and other independent and erroneous irregularities are now minimized by averaging the results, producing the direct response chronology shown in Figure 7. The error associated with this averaging is ±3000 yr. As discussed previously, it is an underestimate.

To compute the related overestimate we must determine the overall (smoothed) trend of this averaged result. In RC11-120 this trend appears to be a linear slope containing a slight offset at 6-m depth in the core. Evidence obtained by W. Prell (personal communication, 1983) indicates that the offset at 6 m was mechanically introduced. Indeed, at 6-m depth is the junction of two core pipes—a potential and common source of mechanical offset introduced by the core extrusion process. Assuming this to be the case, there is no a

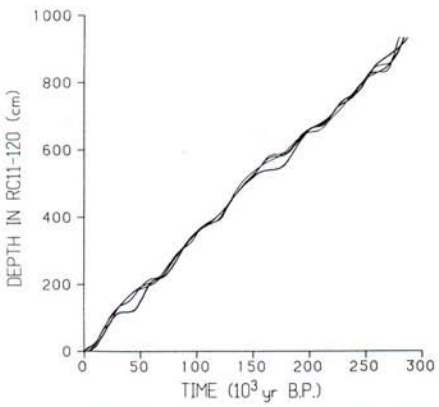

FIG. 6. Superimposed age models from Figure 5a after normalization in time to remove systematic lags between them and the result showing the minimum absolute lag to the forcing (= *C. davisiana*).

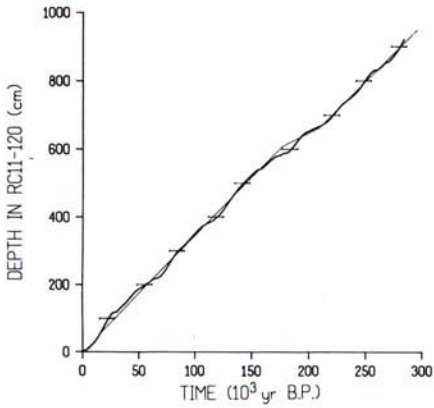

FIG. 7. Direct response approach chronology, from averaging the four chronologies of Figure 6. Error bars have magnitude −7500 to +5000 yr. Linear trend represents an eyeball fit to overall trend of the result.

priori reason for suspecting that an actual change in sedimentation rate occurred across the offset. The linear trend is thus drawn (Fig. 7) using an eyeball fit (and adjusted to zero the mean difference) so that the slope of the two segments is equal. The magnitude (root mean square) of the perturbations about this trend is ~3000 yr. Since this overestimate is the same as the ±3000-yr underestimate, the best estimate for the error related to the quality of the underlying assumption is ±3000 yr.

Finally, the minimum response parameter (*C. davisiana*) leads $\delta^{18}O$ by 2500 yr while $\delta^{18}O$ has a 5000-yr (modeled) absolute lag. So, the systematic error associated with assuming that the minimum response parameter represents an instantaneous response is −2500 yr. Combining this with the 3000-yr error discussed above and the ±1750-yr error associated with our use of the July irradiation curve yields a total error range of −7500 to +5000 yr.

NONLINEAR RESPONSE APPROACH

Assumptions and Potential Error Sources

Irregularities (i.e., perturbations about the linear trend) present in the direct response chronology (assuming the error involved in determining the phase relationship of the forcing is fairly small, as indicated) essentially reflect (1) actual change in sedimentation rate and/or (2) errors resulting from the forced overtuning of extraneous variance (i.e., signal arising from nonlinear and/or nonorbital effects). Those perturbations resulting from not accounting for the nonlinear response of the climate signal should be eliminated by correlating the data to a response inclusive of nonlinear effects. In the previous approach the response was assumed to be strictly linear as it simply mimicked the forcing. Here, we try to account for the nonlinear response of the climate system, then correlate the data directly to this nonlinear response. If the proper response is used as the tuning target, we expect an improvement over the previous result in the form of a reduction in the magnitude of the perturbations.

Sources of error for this approach include those related to the degree to which we properly determine the nonlinear climate response and response time, quality of our underlying assumption, and precision with which the data are correlated to the tuning target.

Generation of the proper tuning target requires knowledge of how the nonlinear response manifests itself in the climate signal and the amount of lag, if any, between the forcing and response. The error associated with our estimation of the lag (system response time) is systematic and bounded at the upper limit since the shortest possible response time is instantaneous. A lower limit is estimated from models. These range from simple to complex and thus represent a reasonable sampling from which to make an estimate. They include Birchfield *et al.* (1981), 6000 yr; Weertman (1976), 6000 yr; Imbrie and Imbrie (1980), 5000 yr; Calder (1974), 7500 yr; and Saltzman *et al.* (1984), 5000 yr. Owing to the small scatter, we average these values to obtain a representative estimate of 6000 yr. These limits therefore suggest that the chronology determined in this approach should lie between the (instantaneous) direct response chronology and a chronology as much as 6000 yr younger.

As before, errors associated with the quality of our underlying assumption arise through overtuning (forcing a match between the data, which contains nonorbitally related variance, and a tuning target which does not). This introduces noise (perturbations) into the age model, as does tuning to a target in which the nonlinear component has been improperly modeled. Therefore, the magnitude of these two sources of error is estimated together, by determining the magnitude of the perturbations about a smoothed trend of the resulting chronology. Minor perturbations introduced by miscorrelation are again included in this estimate.

We use the nonlinear climate response curve from the Imbrie and Imbrie (1980) model as our tuning target. This model offers a distinct advantage because its forcing function is the 65°N, July irradiation curve—the curve used as the direct response approach tuning target. This model thus allows us to isolate the effects of the nonlinear response on the chronology itself. That is, correlation of the model output to the irradiation input yields a mapping function (Fig. 8) whose only perturbations about a linear slope are a result of the nonlinearity introduced by the model (and any miscorrelation). The magnitude of these perturbations provides an estimate of the nonlinear related noise in the direct response approach. Also, by comparing the distribution of the perturbations (along the abscissca) to those present in the $\delta^{18}O$ direct response chronology, we estimate whether or not the nonlinearity introduced by this specific model is consistent with that present in the data.

As seen, the major hiatuses present in the mapping function (Fig. 8) at approximately 0, 70,000, 170,000, and 270,000 yr are present (slightly offset in some instances) in the direct response chronology as well. These features correspond to the 100,000-yr eccentricity cycle introduced by the nonlinearity of the model. These similarities suggest that the model has, to some degree, introduced nonlinearities in a

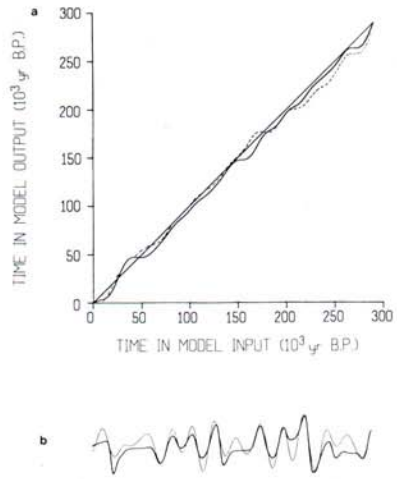

FIG. 8. (a) "Mapping" function (solid line) which relates output curve from the Imbrie and Imbrie (1980) nonlinear climate response model to the model input. Curve represents effects introduced into age models due to nonlinear response of the climate system. Dashed curve represents direct response chronology from Figure 5 for the oxygen-isotope record. (b) Correlation between the model output (bold) and input (light) curves as dictated by above mapping function.

manner consistent with the data. The smaller perturbations reflect nonlinear effects of a much smaller scale with magnitude no larger than those introduced by miscorrelation (induced by the nonlinearity). The systematic offset of the mapping function from the linear slope in Figure 8 reflects the 5000-yr system response time of this model (for the $\delta^{18}O$ record). From this, the error related to the uncertainty in the system response time is -1000 to $+2500$ yr (i.e., the model introduces 5000 of our previously estimated 6000-yr lower limit, and since the $\delta^{18}O$ record lags the minimum response parameter by 2500, the 5000-yr lag built into the tuning target may overestimate the system response by no more than 5000–2500 yr to remain causal).

Implementation

The oxygen-isotope record is correlated to the Imbrie and Imbrie model to produce the nonlinear response chronology (Fig. 9) which should include a minimal amount of noise attributed to nonlinear effects. In

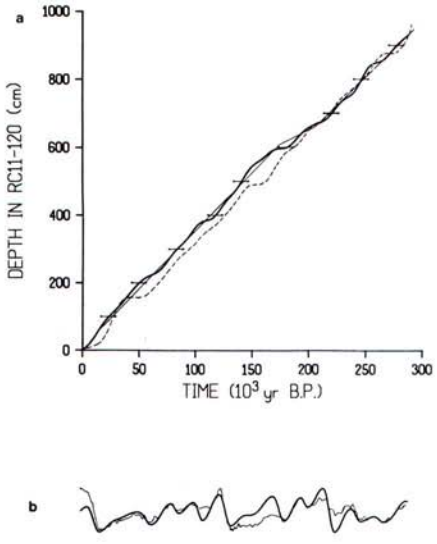

FIG. 9. (a) Chronology resulting from the nonlinear tuning approach. Error bars have magnitude −4000 to +5500 yr. Linear trend represents an eyeball fit to overall trend of the result. Dashed curve is mapping function from Figure 8a for comparison. (b) Correlation between $\delta^{18}O$ data record (bold) and the nonlinear climate response curve (light) produced by the Imbrie and Imbrie (1980) model.

fact, the noise reduction should coincide with the major perturbations present in the mapping function of Figure 8, representing the nonlinear effects introduced by the model. Indeed, the two results, when superimposed (Fig. 9), still show some similarity but most of the major "apparent" hiatuses introduced by the nonlinear effects appear to be reduced. The remaining perturbations therefore represent actual sedimentation rate changes, nonorbital components or nonlinear effects not modeled by this particular model, as well as slight irregularities due to any miscorrelation.

The error related to the magnitude of the perturbations about the smoothed trend (established in the previous approach) is ±3000 yr—the same as that in the direct response approach. This reflects the advantage of using four different climatic indicators in that approach to reduce the perturbations associated with any one particular recording. In this approach, a simila reduction is obtained by including the no linear effects in the tuning target for single parameter. The reduction is not sub stantial though, suggesting that the no linear effects may not play as major a rol in the actual timing of events as they do i the shape of them.

The ±3000-yr error above, combine with the −1000- to +2500-yr error asso ciated with our uncertainty in the syste response time, results in a total error o −4000 to +5500 yr.

PURE COMPONENTS APPROACH

Assumptions and Potential Error Sources

The final tuning approach avoids error associated with RC11-120 by using th stacked $\delta^{18}O$ record of Pisias *et al.* (1984 directly. This approach involves a tunin target constructed from the linear combina tion of "pure" components—the orbita components and their harmonics. The phases and amplitudes of the orbital com ponents are determined in a manner simila to that used in the phase lock approach. The harmonic components are determined by implementing the approach in an itera tive manner. That is, we begin by con structing the tuning target using only the frequency components of obliquity and precession taken directly from the Milan kovitch theory. After tuning to this target, the data are spectrally analyzed for orbital harmonics which are added to the tuning target. Since the final target contains har monics as well as pure orbital components, it implicitly assumes a nonlinear response.

Sources of error for this approach in clude those related to the accuracy with which the phases of the components are determined, the quality of the underlying assumption, and the precision with which the data are successfully correlated to the tuning target. The phase related error is es timated, as in the phase locked approach, from the data using the independent chro nology of Hays *et al.* (1976).

The error related to the quality of the un-

derlying assumption is essentially limited to the fact that extraneous variance is not fully modeled. As in the previous two approaches, this error is manifested through overtuning. An estimate of the magnitude of this error is made in the standard way by measuring the amplitude of the perturbations about the overall (smoothed) trend. This estimate includes error introduced due to miscorrelation of the data to the tuning target as usual.

Implementation

The amplitudes and phase of the orbital components comprising the tuning target are determined from the data (the stacked $\delta^{18}O$ record) using the initial (ELBOW) chronology from Hays *et al.* (1976). In this case the phases, determined over the entire length of the signal, are 9000 ± 3000 yr for obliquity and 1000 ± 3500 yr for the 23,000-yr precessional component (which fixes the phase of the 19,000-yr component as well). These components are combined with a relative amplitude so as to produce a record looking most similar to the data. The initial time scale is then determined by correlating the data to this tuning target (similar to the direct response approach).

Spectral analysis of this initially tuned record reveals harmonics at 11,500- and 15,000-yr periods. These harmonics are coherent with the true harmonics and thus included here. All four components are now combined; their relative amplitudes and phase are taken from the spectrum. The orbital phases, though, are adjusted within the error estimates to produce a tuning target (Fig. 10) most similar in shape to the data record. This results in phases of 6000 and 2000 yr for the obliquity and 23,000-yr precessional components, respectively.

The data are correlated to the tuning target and presented in Figure 11. As seen, the determination of an overall trend is more difficult for this record than for the record of RC11-120. Therefore, this result is transferred to RC11-120 before estimating the magnitude of the perturbations

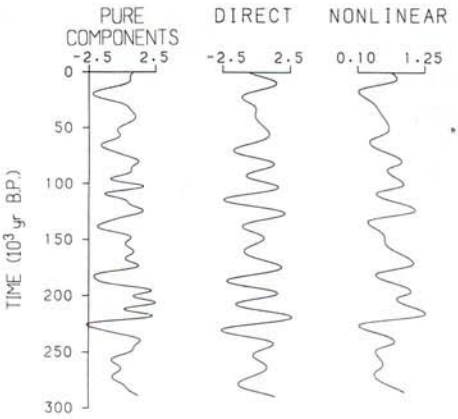

FIG. 10. Tuning target constructed for the pure components tuning approach (leftmost curve) as well as those for the direct response and nonlinear response tuning approaches for comparison (arbitrary scale for the ordinate).

about the trend. This also allows us to be consistent in our estimate of the error.

The transfer is made by correlating the stacked isotope record to the $\delta^{18}O$ record of RC11-120. However, the $\delta^{18}O$ signal in the stacked record is based upon benthic

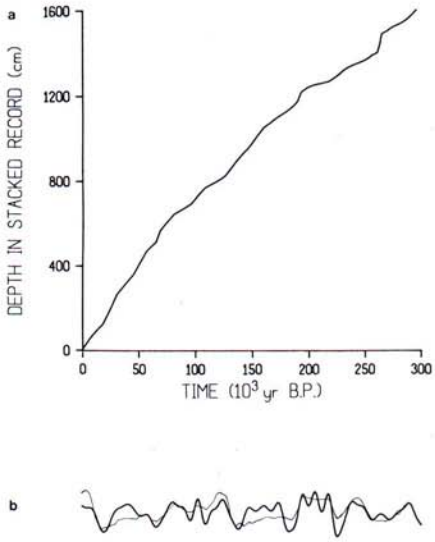

FIG. 11. (a) Chronology in the stacked isotope record resulting from the pure components tuning approach. (b) Correlation between stacked isotope record (bold) and pure components tuning target (light).

foraminifera whereas the RC11-120 benthic $\delta^{18}O$ record extends only one third the length of the core owing to a paucity of benthic forams. Therefore, the transfer over the lower (older) two thirds of the record must be made by correlating the stacked benthic $\delta^{18}O$ record to the RC11-120 planktonic $\delta^{18}O$ record. This introduces an error related to subtle differences between the benthic- and planktonic-derived $\delta^{18}O$ signals.

An estimate of the magnitude of this error is obtained by correlating the benthic- and planktonic-derived $\delta^{18}O$ records of RC11-120 to one another. Because these signals are from the same core, the correlation between them should be described by a simple straight-line mapping function (representing a one-to-one correlation between the data points in the two records). Differences between the two signals, though, manifest themselves as perturbations about this straight line, and the magnitude of these provides an estimate of the error involved in correlating a benthic- to a planktonic-derived oxygen-isotope curve. In this manner, we determine the magnitude of this error to be ~1000 yr (applicable to the older two thirds of the transferred chronology only).

The correlation between the stacked and RC11-120 $\delta^{18}O$ records is extremely good (Fig. 12) and the chronology is thus transferred to RC11-120 using the mapping (or transfer) function of Figure 12a. As estimated in the next section this transfer is accurate to approximately a single sampling interval which spans ~1500 yr in RC11-120. This error estimate is computed in such a way that it includes the ±1000-yr error related to correlating a benthic to a planktonic $\delta^{18}O$ record. Also, while this error must be included in transferring this (and the final) chronology to another record, it will contribute to increasing the magnitude of the perturbations about the overall trend. Thus, in this case this error is included in the error estimate derived from the magnitude of these perturbations.

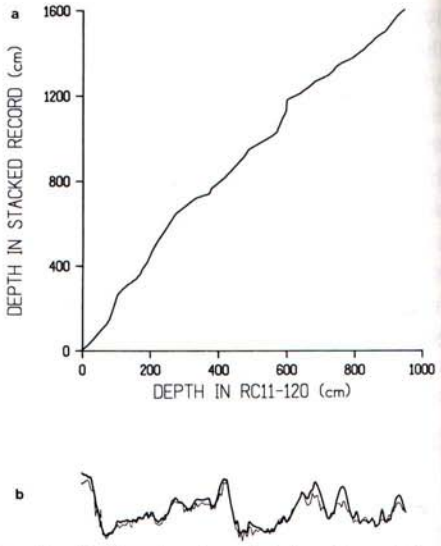

FIG. 12. (a) Mapping (transfer) function relating the stacked oxygen-isotope record to that of RC11-120. Upper third of RC11-120 record is $\delta^{18}O$ from benthonic foraminifera, lower two thirds from planktonic foraminifera. (b) Correlation between stacked record (light) and isotope record of RC11-120 (bold) as dictated by above mapping function.

The pure components chronology after its transfer to RC11-120 is shown in Figure 13. The magnitude of the perturbations about the smooth trend is ~4500 yr. Combined with the ±3500-yr error related to the uncertainty in the highest frequency primary component (precession) it produces a total potential error of ±8000 yr.

FINAL CHRONOLOGY AND ITS TRANSFER

Combining the Results

The chronologies from each of the four orbital tuning approaches are now compared to reveal the degree of overall convergence (Fig. 14). As seen, the convergence is quite good, especially given the variety of assumptions, climatic records, and tuning targets used to obtain the individual results. This convergence implies that the result is fairly insensitive to the tuning approach used.

We now determine the most appropriate

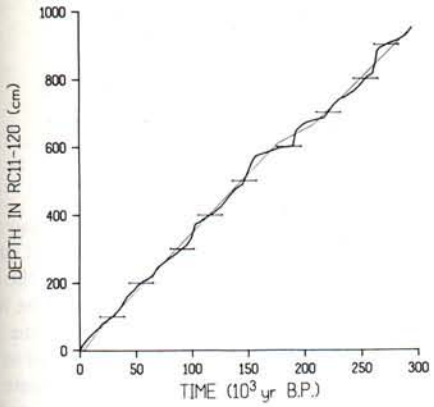

FIG. 13. Pure components chronology after transfer to RC11-120 using transfer function of Figure 12a. Error bars have magnitude 8000 yr. Linear trend represents an eyeball fit to overall trend of the result (slope of this trend is the same as that in the previous two age model results).

manner in which to combine (or choose amongst) these results in an effort to establish a single chronology. Since each chronology should have a nearly independent set of associated errors, an averaging of the various results may offer the best solution. In particular, averaging serves to enhance the true chronology while reducing the uncorrelated error and it allows two independent estimates for the error associated with the resulting (averaged) chronology. First, the averaging itself has an associated error reflecting the degree of convergence. Second, the absolute errors for each chronology are averaged and then reduced by a factor of $1/\sqrt{n}$ where n is the number of chronologies averaged. The difference in magnitude between these two estimates provides an additional measure of the quality of the overall error estimates and thus of the achieved result itself. As we have no other criteria for choosing an alternate method of combining the results, or choosing a best result from the four available, this averaging procedure offers the most unbiased choice and the smallest magnitude errors. Furthermore, by invoking no other criteria we maintain our dependence on a single underlying assumption: that the metronome is present to some extent in the data records.

The averaged chronology (averaging time, at 1-cm depth intervals) is presented in Figure 15 (values in Appendix). The errors associated with the individual chronologies are averaged and reduced by $1/\sqrt{n}$ ($=0.5$) to give an error estimate for the averaged chronology of magnitude of ~3500 yr (including systematic errors). The

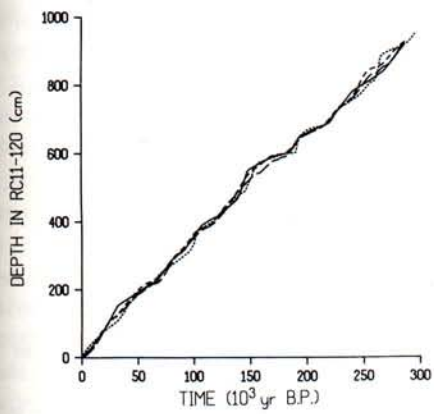

FIG. 14. Comparison of all four age models. Solid (bold) result is that from phase locked approach. Long dashed result from direct response approach. Dotted result from pure components response approach. Short dashed result from nonlinear approach.

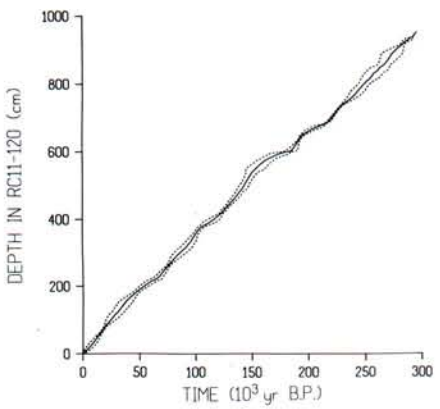

FIG. 15. Final chronology (as it appears in RC11-120) based on average of four results presented in Figure 14. Error envelope has average magnitude of 3500 yr. Error associated with standard deviation of the four individual results about this average is ±2500 yr.

average magnitude of the error (standard deviation) reflecting the degree of convergence is 2500 yr. This represents an excellent agreement with the first estimate, and helps to instill a confidence in its magnitude and produced chronology.

We combine these two independent estimates of the total error in the following manner. The error associated with the degree of convergence produces an error envelope whose shape reflects the fact that the age estimates at some depths are more reliable than those at other depths. We then scale this envelope so that its average magnitude about the averaged chronology is equal to the absolute ~3500-yr error computed from combining the error estimates from the individual chronologies. The resulting envelope (Fig. 15; values in Appendix) is therefore an estimate of the distribution of the absolute error over the length of the chronology.

Transferring the Chronology

The resolution of this final chronology is quite good and it can now be transferred to the stacked oxygen-isotope stratigraphy of Pisias *et al.* (1984). This transfer is done using the mapping function established in the previous section (Fig. 12), relating RC11-120 to the stacked record. The excellent agreement between the two records using this correlation should assure the accuracy of the transfer. However, in order to test the sensitivity of the chronology to a transfer in this manner, the nonlinear orbital tuning approach is applied directly to the stacked record by correlating it to the Imbrie and Imbrie (1980) model output. This result is compared, in Figure 16, to the nonlinear chronology developed in RC11-120, but transferred to the stacked record via the transfer function of Figure 12. As seen, the two results are extremely similar and agree to within ±1500 yr. The transfer of the chronology to the stacked record is thus assumed to maintain the high integrity

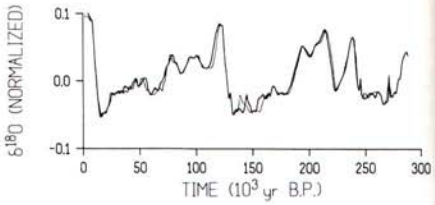

FIG. 16. Comparison of two nonlinear response age models in the stacked isotope record. The bold curve represents the results obtained by developing the age model directly within the stacked record. The light curve is the result obtained by transferring the age model from RC11-120 (where it was developed) to the stacked record via the mapping function of Figure 12. Results agree to within a single sampling interval = 1500 yr.

of the original results. An addition to the magnitude of the error envelope of 1500 yr accommodates the error associated with this transfer process.

The result of the age transfer produces the final chronology of Figure 17 and the standard oxygen-isotope chronostratigraphy of Figure 18. The error envelope about the final chronology has an average (absolute) error of ±5000 yr. The values of these results are tabulated in Table 2. Figure 19 shows the instantaneous sedi-

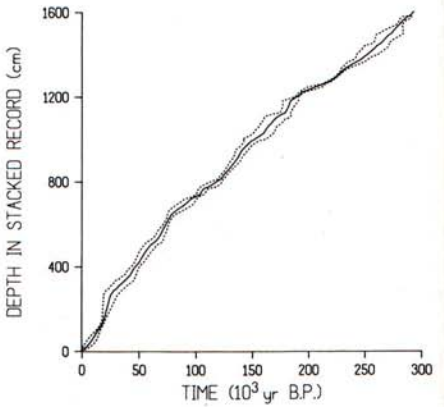

FIG. 17. Final chronology as it appears in the stacked oxygen-isotope record obtained by transferring the results of Figure 15 from RC11-120 using the mapping function of Figure 12. Error envelope has average magnitude of 5000 yr.

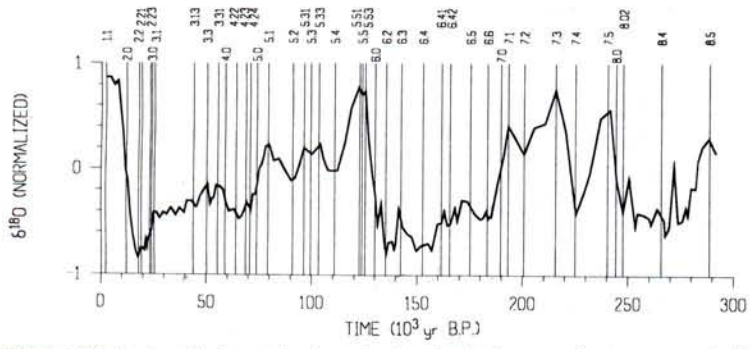

FIG. 18. Final orbitally based chronostratigraphy (= stacked oxygen-isotope record of Pisias *et al.*, 1984, with the chronology of Figure 17 as a time base). Numbered vertical lines indicate identifiable features of the record, defined by Pisias *et al.* (1984). Age estimates for these features are given in Table 2. Descriptions of the features are given in Pisias *et al.* (1984; their Table V).

mentation rates resulting from this final chronology.

DISCUSSION AND CONCLUSION

We have used the concept of orbital tuning to construct a high-resolution chronostratigraphy whose stratigraphic foundation is based on the equally high-resolution oxygen-isotope stratigraphy of Pisias *et al.* (1984). The actual construction involved several different assumptions (outlined in Table 1) as to how the orbital signal, or metronome, is embedded within the geological climate record and, therefore, how it should be isolated and/or adjusted to remove variations in the rate at which it was recorded. In this manner we have been able to test the sensitivity of orbital tuning to the actual orbital tuning technique used, while simultaneously assessing the magnitude of the error associated with such a chronological development. The results have been highly successful and suggest that the age model produced is fairly insensitive to the tuning technique employed. Furthermore, the magnitude of the associated absolute error is consistently small throughout the ~300,000 yr of the record used. This error has been computed as being ±3500 yr with an additional 1500-yr error related to the process of transferring the chronology to a different isotope record. This error is of similar magnitude to that estimated in an independent manner and is related to the degree of convergence of the individual chronologies produced from the different tuning strategies. This provides independent support for the magnitude of the errors presented and allows us to estimate how the absolute error is distributed with age.

To aid in its evaluation, the age estimates obtained in our final chronology are compared to a variety of age estimates made previously. Ages for the last interglacial have been made using $^{230}Th/^{234}U$ based measurements on raised coral terraces. Dates for terraces corresponding to our events 5.1 (79,250 yr; stage 5a), 5.33 (103,290 yr; stage 5c), and 5.51–5.53 (122,560–125,190 yr; stage 5e) have been given for New Guinea (Bloom *et al.*, 1974): 82,000, 103,000, and 124,000 yr; Barbados (Fairbanks and Matthews, 1978): 82,000, 105,000, and 125,000 yr; and Haiti (Dodge *et al.*, 1983): 81,000, 108,000, and 130,000 yr. Mix and Ruddiman (1986, Fig. 3) show the last glacial maximum (our event 2.2; 17,850 yr) having a ^{14}C age ranging from 13,000 to 19,000 yr. These radiometric ages agree quite well with our orbitally derived ones.

Imbrie *et al.* (1984) developed an orbitally based chronology for an 800,000-yr $\delta^{18}O$ stacked record. They used a single

TABLE 2. AGE ESTIMATES, BASED ON THE FINAL CHRONOLOGY DETERMINED FOR THE STACKED ISOTOPE RECORD OF PISIAS *ET AL.* (1984)

Event[a]	Depth (cm)	Age (yr)	Error (yr)	$\delta^{18}O$ (normalized)	Event[a]	Depth (cm)	Age (yr)	Error (yr)	$\delta^{18}O$ (normalized)
	2.6	210	1070	0.92		313.6	33,210	6970	-0.38
1.1	13.0	2320	2110	0.86		324.0	35,560	7280	-0.45
	13.8	2480	2200	0.86		334.5	37,370	7740	-0.38
	22.3	4200	3050	0.86		344.8	39,690	6690	-0.43
	34.4	6270	3730	0.78		354.2	41,000	6210	-0.31
	44.5	7810	4020	0.82		364.5	42,930	4970	-0.31
	54.7	9140	3990	0.53	3.13	375.0	43,880	4710	-0.34
	64.5	10,310	3760	0.31		375.7	43,940	4690	-0.34
	74.6	11,440	3390	0.00		385.3	44,820	4500	-0.37
2.0	80.0	12,050	3140	-0.06		392.2	45,570	4280	-0.37
	84.7	12,580	2930	-0.12		404.4	47,300	3610	-0.26
	94.5	13,700	2420	-0.42		414.6	48,900	3520	-0.21
	105.3	14,990	1850	-0.62	3.3	423.0	50,210	3850	-0.17
	114.6	16.160	1480	-0.77		424.2	50,390	3900	-0.16
	123.5	17.310	1400	-0.85		434.6	51,570	4210	-0.36
2.2	129.0	17,850	1370	-0.84		444.6	52,670	4450	-0.29
	133.7	18.310	1340	-0.83		453.7	53,690	4660	-0.28
	144.7	19,130	1370	-0.76		463.8	54,840	4910	-0.16
2.21	146.0	19,220	1390	-0.76	3.31	469.0	55,450	5030	-0.17
	152.8	19,690	1470	-0.76		474.2	56,050	5150	-0.17
	164.4	20,330	1860	-0.77		485.2	57,600	5430	-0.20
	174.4	20,860	2270	-0.79		494.8	58,930	5560	-0.32
	184.7	21,400	2720	-0.71	4.0	495.0	58,960	5560	-0.32
	194.9	21,940	3170	-0.79		504.9	60,440	5680	-0.41
	203.4	22,380	3540	-0.70		515.1	62,970	6590	-0.39
	212.6	22,850	3930	-0.66	4.22	520.0	64,090	6350	-0.43
2.23	219.0	23,170	4190	-0.65		525.0	65,220	6110	-0.48
	222.8	23,360	4340	-0.65		534.9	66,970	5000	-0.45
	234.3	23,930	4790	-0.60		544.8	68,250	4350	-0.39
3.0	238.0	24,110	4930	-0.60	4.23	550.0	68,830	4200	-0.35
	245.1	24,460	5190	-0.59		553.2	69,190	4120	-0.33
	253.4	24,860	5490	-0.49		564.0	70,240	4040	-0.37
	263.3	25,350	5870	-0.42	4.24	570.0	70,820	3950	-0.40
3.1	264.0	25,420	5900	-0.42		573.1	71,120	3910	-0.42
	274.8	26,500	6330	-0.42		583.5	72,230	3370	-0.25
	285.2	27,950	6660	-0.48		593.4	73,250	2870	-0.25
	294.2	29,730	6580	-0.42	5.0	600.0	73,910	2590	-0.18
	302.9	31,450	6660	-0.44		604.3	74,340	2410	-0.14

[a]Events are those indicated in Figure 18. Additional events frequently appear in high resolution records see Pisias et al. (1984; their Table II). Error estimates given are for the error envelope of Figure 17. These reflect an estimate as to how the ±5000 yea absolute error is distributed over the length of the chronology.

TABLE 2—*Continued*

Event[a]	Depth (cm)	Age (yr)	Error (yr)	$\delta^{18}O$ (normalized)	Event[a]	Depth (cm)	Age (yr)	Error (yr)	$\delta^{18}O$ (normalized)
	614.2	75,320	2160	0.00		912.1	136,590	4150	-0.70
	624.9	76,370	2170	0.04		923.5	137,970	3900	-0.69
	634.7	77,310	2450	0.10		933.5	139,020	4190	-0.78
	644.7	78,300	2920	0.21		942.4	139,980	4720	-0.73
5.1	651.0	79,250	3580	0.22		954.1	141,330	5580	-0.41
	653.7	79,660	3870	0.22	6.3	959.0	142,280	5280	-0.50
	663.6	81,790	5270	0.07		961.7	142,810	5120	-0.55
	673.5	84,130	6200	0.09		974.0	145,240	4740	-0.62
	681.6	86,310	6670	0.01		983.6	147,110	5150	-0.64
	695.3	90,100	7080	-0.12		994.5	149,340	6290	-0.78
5.2	699.0	90,950	6830	-0.11		1003.5	152,140	9920	-0.73
	704.6	92,230	6440	-0.09	6.4	1005.0	152,580	9910	-0.73
	714.0	94,060	5830	0.02		1013.5	155,090	9870	-0.71
5.31	724.0	96,210	5080	0.18		1020.0	157,100	9290	-0.78
	724.8	96,380	5020	0.19		1030.7	159,890	9050	-0.52
5.3	733.0	99,380	3410	0.14	6.41	1041.0	161,340	8860	-0.51
	734.6	99,960	3100	0.13		1044.5	161,830	8800	-0.51
5.33	743.0	103,290	3410	0.21		1053.5	162,790	8490	-0.42
	744.3	103,800	3460	0.22		1062.3	164,110	8010	-0.54
	754.4	105,080	3740	0.10	6.42	1069.0	165,350	8390	-0.53
	763.1	106,050	4000	0.04		1072.5	165,990	8590	-0.52
	772.6	107,550	4510	-0.02		1082.7	167,770	9280	-0.39
5.4	780.0	110,790	6280	-0.02		1090.0	168,890	9200	-0.52
	783.4	112,280	7100	-0.02		1103.0	171,370	10,430	-0.30
	795.0	115,910	6280	0.25		1112.5	173,670	10,970	-0.31
	804.4	118,690	4910	0.57	6.5	1117.0	175,050	9840	-0.36
	816.0	122,190	2350	0.76		1123.0	176,900	8330	-0.42
5.51	818.0	122,560	2410	0.74		1130.0	179,730	4690	-0.48
	824.7	123,790	2610	0.69		1141.5	180,910	4750	-0.47
5.5	825.0	123,820	2620	0.69		1150.0	181,700	4910	-0.45
	834.8	125,000	2960	0.72		1160.0	182,640	5100	-0.41
5.53	836.0	125,190	2920	0.66	6.6	1170.0	183,300	5740	-0.48
	844.6	126,580	2640	0.27		1171.0	183,370	5810	-0.49
	855.3	128,310	2670	-0.04		1183.5	184,170	6720	-0.45
	864.1	129,700	3020	-0.25		1190.0	185,190	6260	-0.46
6.0	865.0	129,840	3050	-0.28		1200.0	188,290	3240	-0.14
	873.3	131,090	3360	-0.57	7.0	1205.0	189,610	2310	-0.02
	884.9	132,810	3730	-0.37		1210.5	191,080	1290	0.12
	894.9	134,230	4090	-0.71	7.1	1220.0	193,070	2020	0.38
6.2	901.0	135,100	4240	-0.80		1220.5	193,180	2060	0.39
	902.7	135,340	4290	-0.83		1230.5	196,070	3080	0.29

TABLE 2—*Continued*

Event[a]	Depth (cm)	Age (yr)	Error (yr)	$\delta^{18}O$ (normalized)	Event[a]	Depth (cm)	Age (yr)	Error (yr)	$\delta^{18}O$ (normalized)
7.2	1240.0	200,570	4960	0.13		1422.0	257,180	10,160	−0.43
	1250.0	205,530	6350	0.39		1434.5	259,820	10,730	−0.46
	1260.0	210,800	4030	0.43		1440.0	260,680	10,860	−0.54
7.3	1270.0	215,540	1420	0.73		1452.3	263,900	8160	−0.38
	1281.7	220,140	1770	0.35	8.4	1460.0	265,670	7720	−0.44
	1290.0	222,520	1360	−0.05		1464.5	266,700	7450	−0.48
7.4	1299.0	224,890	1210	−0.40		1470.0	267,480	7810	−0.64
	1300.0	225,160	1190	−0.44		1483.3	269,820	9540	−0.55
	1311.5	227,360	1220	−0.32		1494.0	271,680	11,010	−0.04
	1323.0	229,790	1510	−0.19		1500.0	273,420	10,960	−0.51
	1334.0	231,850	2500	−0.05		1514.0	275,840	8650	−0.49
	1340.0	233,200	3390	0.08		1524.0	277,360	7070	−0.38
	1350.5	237,030	4920	0.48		1530.0	278,370	5850	−0.47
7.5	1359.0	240,190	6340	0.53		1540.0	280,160	3710	−0.18
	1361.7	241,190	6780	0.55		1553.0	282,330	2480	−0.19
8.0	1370.0	244,180	7110	−0.11		1560.0	283,330	2650	0.08
8.02	1380.0	247,600	6250	−0.43		1571.0	285,340	4000	0.21
	1392.5	250,370	6950	−0.12		1584.0	288,170	3960	0.28
	1404.5	253,430	9610	−0.58	8.5	1585.0	288,540	3520	0.27
	1410.0	254,620	9870	−0.42		1593.0	291,460	0	0.15

tuning technique similar to our phase-locked approach. Despite the lower resolution of their significantly longer record, comparison of the younger portion of their chronology with that developed here shows that all ages agree to within the error bars [note that events 8.4 and 8.5 were incorrectly labeled 8.2 and 8.3 in Pisias *et al.* (1984) relative to the labeling of the Imbrie *et al.* (1984) events and have been corrected here]. Since our analysis indicates that the tuned result is fairly insensitive to the actual tuning technique and climatic indicator used, the Imbrie *et al.* (1984) long time scale results are reinforced by those obtained here. Therefore, we suggest that for short (<300,000 yr), high-resolution data sets, the high-resolution chronology developed here is most applicable. For longer records, the Imbrie *et al.* (1984) chronology is the obvious choice.

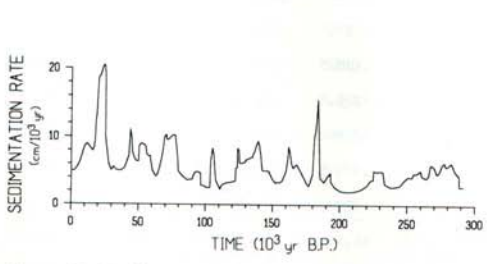

FIG. 19. Sedimentation rate of stacked record based on final chronology.

Based on our chronology, we now determine an estimate for the amount of variance in the $\delta^{18}O$ climate record which can be attributed to a linear response to the orbital forcing.[3] As previously discussed, Mi-

[3] The estimate for the total amount of described variance is achieved by computing the square of the correlation coefficient between the $\delta^{18}O$ record in time and the orbital forcing curve. The estimate for the described variance in a narrow frequency band is given by the squared coherence value for the frequency band of interest.

lankovitch considered obliquity and precession to be the driving components in the orbital forcing. Fully 80% of the $\delta^{18}O$ variance distributed in the frequency range of these two orbital components can be described as a linear response to such an orbital forcing. But, only 25% of the complete $\delta^{18}O$ record can be described as a linear response to this forcing. If the 100,000-yr eccentricity component is included in the orbital forcing (it was not used for tuning), the total variance described by a linear response is ~50%, and 72% of the variance in the frequency range of eccentricity can be described by a linear response to the eccentricity component. Therefore, the data suggest that about 50% of the climate response (as recorded by the $\delta^{18}O$ record) can be described by a simple linear response to orbital forcing. The remaining signal variance is unaccounted for by this simple model and requires further investigation.

Finally, the results obtained here have obvious implications. Most importantly they demonstrate that orbital tuning techniques can provide consistent and seemingly reliable (based on a comparison to radiometric dates) age estimates. Because this chronology is for a globally representative climatic record, any investigator can transfer these ages to his own $\delta^{18}O$ record(s) and establish a standard and consistent chronostratigraphy from which individual time slices or entire records can be compared and evaluated.

APPENDIX

Depth, Age, Error, and Values for Various Climatic Indicators Measured in Core RC11-120

Depth (cm)	Age (yr)	Error (yr)	Planktonic $\delta^{18}O$ (per mil)	Benthonic $\delta^{18}O$ (per mil)	*Cycladophora davisiana* (%)	Ts (°C)	$\delta^{13}C$ (per mil)	Calcium carbonate (%)
2	750	410	-	-	-	11.2	-	72.2
5	1810	910	1.87	3.33	-	-	0.92	-
10	3350	1420	1.96	3.29	0.89	11.5	0.73	68.9
15	4730	1720	1.97	3.24	-	-	0.87	-
20	6090	1940	1.96	3.29	1.19	10.6	0.74	77.1
25	7410	2090	2.16	3.58	-	-	0.64	-
30	8640	2130	2.38	3.62	1.46	13.2	0.60	73.5
35	9790	2050	2.32	3.66	-	-	0.56	-
40	10,910	1890	2.60	4.52	-	-	0.35	71.8
45	12,010	1670	2.74	4.15	-	-	0.41	-
50	13,110	1420	2.98	4.45	3.72	9.1	0.36	63.7
52.5	13,670	1280	-	4.98	-	-	-	-
55	14,220	1150	2.95	4.23	-	-	0.57	-
60	15,340	900	3.37	5.14	13.56	7.0	0.57	48.6
65	16,460	750	3.28	5.11	-	-	0.64	-
70	17,570	740	3.53	5.27	10.14	7.0	0.52	44.5
75	18,520	710	3.34	5.22	-	-	0.61	-
80	19,530	740	3.36	5.11	16.61	7.1	0.61	36.3
85	20,740	1150	3.43	5.10	-	-	0.57	-

APPENDIX—*Continued*

Depth (cm)	Age (yr)	Error (yr)	Planktonic $\delta^{18}O$ (per mil)	Benthonic $\delta^{18}O$ (per mil)	Cycladophora davisiana (%)	Ts (°C)	$\delta^{13}C$ (per mil)	Calcium carbonate (%)
90	21,980	1690	3.34	5.04	15.25	7.4	-	-
91	22,230	1800	-	-	-	-	-	40.8
95	23,240	2240	3.31	4.88	-	-	0.87	-
100	24,510	2760	3.29	-	9.78	7.0	0.86	42.9
105	25,800	3230	3.32	4.78	8.68	7.6	0.96	-
109	26,730	3370	-	-	-	-	-	53.6
110	26,960	3400	3.22	4.89	10.64	7.6	0.96	-
115	28,160	3530	3.07	4.83	7.22	7.6	0.74	-
120	30,010	3420	3.04	4.76	7.72	7.2	0.81	58.95
125	31,290	3500	3.07	4.80	5.65	7.8	0.84	-
129	32,200	3570	-	-	-	-	-	58.87
130	32,430	3590	3.19	4.79	5.88	7.8	0.80	-
135	33,590	3720	2.96	4.64	4.46	8.3	0.75	-
140	34,720	3770	3.11	4.75	3.44	8.0	0.78	62.5
145	35,840	3870	2.98	4.89	2.87	8.7	0.71	-
150	37,020	4050	3.05	4.61	3.56	8.6	0.84	64.9
155	38,130	4040	3.01	4.68	7.02	8.6	0.69	-
160	39,490	3560	2.94	4.72	7.97	9.0	0.62	69.1
165	41,190	3230	2.98	4.62	9.27	9.3	0.75	-
170	42,670	2660	2.95	4.54	4.96	8.2	0.62	64.9
175	44,400	2420	2.89	4.60	6.56	7.8	0.63	-
180	46,070	2130	2.90	4.59	12.57	7.0	0.59	68.7
185	47,750	1860	2.66	4.52	8.57	7.4	0.51	-
189	49,230	1890	-	-	-	-	-	70.4
190	49,620	1930	2.86	4.42	9.12	7.0	0.54	-
195	51,620	2230	2.87	4.44	6.46	8.1	0.40	-
200	53,600	2450	2.82	4.47	8.02	8.2	0.46	71.1
205	55,640	2670	2.82	4.46	5.70	8.2	0.35	-
210	57,910	2880	3.03	4.48	4.08	9.0	0.34	71.4
215	59,980	2970	2.76	4.75	6.04	8.3	0.29	-
220	63,160	3540	3.08	4.76	12.69	7.0	0.39	64.0
225	65,930	3020	3.15	4.81	15.99	7.0	0.71	-
230	67,660	2420	2.84	4.76	11.41	7.0	0.78	62.3
235	68,990	2190	2.98	4.76	10.85	8.1	0.79	-
240	70,160	2130	2.85	4.53	6.89	7.2	0.81	68.0
245	71,340	2010	2.82	4.42	4.17	7.6	0.81	-
250	72,640	1670	2.71	4.42	3.59	8.1	0.87	72.3

APPENDIX—*Continued*

Depth (cm)	Age (yr)	Error (yr)	Planktonic $\delta^{18}O$ (per mil)	Benthonic $\delta^{18}O$ (per mil)	*Cycladophora davisiana* (%)	Ts (°C)	$\delta^{13}C$ (per mil)	Calcium carbonate (%)
255	73,910	1360	2.59	4.26	4.18	8.8	0.75	-
260	75,190	1150	2.54	-	4.27	7.9	0.88	77.0
265	76,450	1150	2.55	3.92	4.97	8.0	0.89	-
270	77,730	1380	2.59	-	3.49	8.3	0.85	83.3
275	79,020	1790	2.44	-	3.68	8.2	0.78	-
280	80,340	2290	2.43	4.05	4.01	8.3	0.56	81.9
285	81,650	2730	2.42	-	2.91	8.2	0.72	-
290	82,990	3110	2.37	3.98	2.74	10.0	0.50	82.8
295	84,540	3320	2.40	-	2.31	8.1	0.60	-
300	86,160	3500	2.71	-	1.75	7.9	0.67	74.6
305	87,860	3630	2.61	-	2.56	7.1	0.48	-
310	89,630	3720	2.68	-	2.07	7.2	0.73	73.1
315	91,260	3600	2.58	-	3.30	8.3	0.58	-
320	92,560	3330	2.68	-	6.39	7.2	0.69	-
321	92,810	3290	-	-	-	-	-	75.7
325	93,750	3120	2.54	-	4.74	7.6	0.61	-
330	94,890	2950	2.60	-	4.87	8.0	0.57	77.8
335	95,980	2770	2.40	-	4.98	7.4	0.53	-
340	96,950	2460	2.54	-	4.84	7.4	0.62	31.6
345	97,910	2150	2.48	-	3.59	8.1	0.64	-
350	98,870	1880	2.42	-	2.32	8.7	0.51	80.3
355	99,830	1650	2.40	-	1.78	8.3	0.42	-
360	100,820	1500	2.48	-	2.81	9.2	0.58	74.4
365	101,860	1490	2.45	-	2.69	10.0	0.49	-
370	103,000	1640	2.48	-	2.46	8.9	0.52	74.1
375	104,470	1920	2.46	-	3.41	8.3	0.49	-
380	106,890	2270	2.62	-	6.69	7.3	0.61	68.6
385	109,620	2910	2.50	-	5.23	7.1	0.49	-
390	112,050	3760	2.61	-	6.21	8.5	0.57	-
395	114,310	3590	2.42	-	4.46	8.9	0.63	-
400	116,340	3220	2.33	-	3.23	8.9	0.64	73.2
405	118,210	2740	2.14	-	1.15	8.8	0.68	-
410	120,020	2120	2.23	-	0.68	10.2	0.46	-
415	121,860	1350	1.83	-	0.48	9.1	-	-
420	123,390	1240	1.89	-	1.01	9.2	0.49	76.9
425	124,690	1560	1.79	-	0.70	10.1	0.38	-
430	125,960	1450	1.91	-	1.42	13.5	0.34	79.1

APPENDIX—*Continued*

Depth (cm)	Age (yr)	Error (yr)	Planktonic $\delta^{18}O$ (per mil)	Benthonic $\delta^{18}O$ (per mil)	*Cycladophora davisiana* (%)	Ts (°C)	$\delta^{13}C$ (per mil)	Calcium carbonate (%)
435	127,330	1360	2.35	-	0.83	12.3	0.16	-
440	128,710	1450	2.72	-	1.69	13.5	0.17	77.7
445	130,080	1640	2.82	-	1.67	13.6	0.03	-
450	131,390	1810	3.18	-	2.08	9.2	0.17	59.9
455	132,700	1950	3.20	-	1.89	9.0	0.22	-
460	134,040	2130	3.44	-	10.49	7.3	0.18	51.8
465	135,340	2260	3.31	-	10.44	8.3	0.16	-
470	136,490	2210	3.54	-	9.67	7.6	0.34	54.5
475	137,550	2060	3.18	-	8.22	9.1	0.14	-
480	138,750	2150	3.37	-	12.71	7.1	0.25	55.2
485	140,010	2500	3.42	-	12.34	8.0	0.45	-
490	141,250	2960	3.10	-	10.36	7.6	0.41	-
491	141,440	2950	-	-	-	-	-	54.5
495	142,140	2830	3.14	-	7.07	7.9	0.24	-
500	143,010	2660	3.38	-	5.88	7.2	0.28	53.9
505	143,880	2550	3.25	-	2.61	8.7	0.34	-
510	144,760	2500	3.19	-	3.38	8.2	0.33	54.2
515	145,630	2520	3.27	-	1.57	6.2	0.41	-
520	146,500	2610	3.21	-	0.69	7.8	0.37	57.2
525	147,380	2770	3.22	-	1.14	8.0	0.35	-
530	148,270	2980	3.24	-	1.24	8.2	0.18	59.0
535	149,210	3270	3.27	-	1.61	7.4	0.23	-
540	150,340	3800	3.21	-	1.91	7.5	0.25	48.2
545	151,970	5150	3.15	-	1.50	8.8	0.32	-
550	153,270	5360	3.32	-	2.07	7.7	0.22	50.2
555	154,790	5260	3.15	-	1.93	8.8	0.28	-
560	156,550	4970	3.21	-	2.58	7.7	0.34	52.4
565	158,360	4780	3.13	-	4.52	7.7	0.40	-
570	160,150	4770	3.06	-	10.00	8.2	0.39	54.0
575	162,350	4550	2.90	-	12.02	7.7	0.41	-
580	165,210	4200	2.91	-	9.48	7.7	0.28	63.9
585	168,510	4870	2.87	-	9.40	9.3	0.31	-
590	172,110	5910	2.81	-	5.25	7.8	0.35	56.1
595	176,000	4850	2.81	-	9.15	10.0	0.09	-
600	182,760	2700	3.02	-	10.76	7.8	0.20	55.5
605	185,330	3220	2.85	-	16.53	8.3	0.38	-
610	186,520	2580	2.78	-	14.44	8.0	0.15	55.0

APPENDIX—*Continued*

Depth (cm)	Age (yr)	Error (yr)	Planktonic $\delta^{18}O$ (per mil)	Benthonic $\delta^{18}O$ (per mil)	*Cycladophora davisiana* (%)	Ts (°C)	$\delta^{13}C$ (per mil)	Calcium carbonate (%)
615	187,610	2030	2.61	-	8.68	9.2	0.48	-
620	188,560	1580	2.59	-	3.92	8.3	0.62	-
621	188,740	1500	-	-	-	-	-	58.2
625	189,470	1180	2.55	-	2.39	8.7	0.63	-
630	190,380	830	2.43	-	4.99	9.7	0.44	66.7
635	191,310	650	2.32	-	2.65	9.4	0.60	-
640	192,270	810	2.18	-	2.29	9.0	0.53	74.3
645	193,420	1150	2.17	-	2.57	9.8	0.46	-
650	195,020	1410	2.14	-	2.37	10.2	0.31	73.1
655	197,370	1940	2.41	-	2.78	9.0	0.55	-
660	199,830	2450	2.52	-	2.41	7.7	0.71	68.0
665	202,730	2980	2.49	-	2.62	9.3	0.64	-
670	206,110	3390	2.45	-	3.41	7.9	0.63	71.6
675	209,670	2590	2.13	-	3.21	9.7	0.39	-
680	213,290	920	2.31	-	3.28	9.9	0.58	73.5
685	216,300	900	2.24	-	2.02	10.8	0.32	-
690	218,000	1120	2.20	-	1.95	11.5	0.29	70.8
695	219,250	1030	2.47	-	1.89	11.6	0.30	-
700	220,380	910	2.70	-	1.72	8.9	0.37	60.1
705	221,470	800	2.55	-	3.01	8.1	0.15	-
710	222,540	710	2.62	-	3.16	8.1	0.15	57.8
715	223,620	650	2.62	-	4.87	8.9	0.10	-
720	224,730	630	2.86	-	4.58	7.9	0.18	51.3
725	225,930	620	2.85	-	7.96	7.7	0.38	-
730	227,280	640	2.72	-	5.94	8.7	0.23	61.0
735	228,740	700	2.74	-	7.55	8.0	0.38	-
740	230,410	860	2.78	-	10.02	6.9	0.49	58.4
745	232,730	1650	2.46	-	8.53	9.8	0.50	-
750	234,660	2040	2.46	-	8.47	10.9	0.39	67.8
755	236,440	2440	2.45	-	7.31	10.7	0.50	-
760	238,150	2910	2.57	-	4.44	10.7	0.46	75.2
765	239,740	3380	2.38	-	3.67	10.0	0.37	-
770	241,020	3550	2.39	-	2.66	12.0	0.38	80.5
775	242,260	3740	2.62	-	2.62	12.4	0.23	-
780	243,500	3790	2.71	-	2.08	12.0	0.17	75.2
785	244,780	3660	2.67	-	4.65	12.1	0.11	-
790	246,090	3440	2.86	-	6.12	8.7	0.08	65.6

APPENDIX—*Continued*

Depth (cm)	Age (yr)	Error (yr)	Planktonic $\delta^{18}O$ (per mil)	Benthonic $\delta^{18}O$ (per mil)	Cycladophora davisiana (%)	Ts (°C)	$\delta^{13}C$ (per mil)	Calcium carbonate (%)
795	247,410	3290	3.03	-	6.29	8.0	0.01	-
800	248,830	3420	2.92	-	8.78	7.2	0.03	54.6
805	250,240	3630	2.99	-	8.96	8.0	0.00	-
810	251,950	4450	2.94	-	8.62	7.0	-0.10	57.8
815	253,560	5110	-	-	9.50	7.7	0.05	-
820	254,770	5200	2.97	-	7.63	7.3	-0.01	-
821	255,000	5210	-	-	-	-	-	60.7
825	255,950	5260	2.88	-	6.47	7.3	-0.10	-
830	257,230	5360	2.84	-	5.26	7.2	-0.09	61.5
835	259,350	5580	2.91	-	6.31	8.2	-0.04	-
840	260,780	5730	3.04	-	4.99	7.3	-0.01	60.0
845	262,110	5450	2.94	-	6.26	7.7	-0.02	-
850	263,940	4250	2.85	-	3.95	7.8	-0.14	59.3
855	265,960	3740	2.95	-	1.71	7.4	0.16	-
860	267,520	4120	3.15	-	2.83	6.8	-	33.2
865	268,600	4500	-	-	5.46	8.0	0.18	-
870	269,610	4930	-	-	6.16	7.3	-	31.9
875	270,580	5380	-	-	5.10	7.5	-	-
880	271,530	5800	2.91	-	7.53	8.5	-	37.7
885	272,650	5820	-	-	10.83	8.0	-	-
890	273,800	5730	3.00	-	13.39	7.9	-	47.5
895	275,420	4750	2.91	-	13.56	8.5	0.75	-
900	276,920	3990	2.79	-	10.91	6.8	0.79	-
901	277,250	3790	-	-	-	-	-	62.4
905	278,650	2900	2.80	-	7.45	7.8	0.72	-
910	280,560	1730	2.58	-	7.54	8.2	0.40	66.7
915	282,310	1310	2.56	-	7.82	8.3	0.73	-
920	283,520	1540	2.57	-	7.61	7.7	0.75	-
921	283,850	1680	-	-	-	-	-	77.5
925	286,010	2220	2.43	-	6.05	8.4	0.64	-
930	287,790	2220	2.43	-	4.69	8.8	0.56	80.6
935	290,600	0	2.50	-	3.43	9.2	0.52	-
940	291,780	0	2.67	-	3.95	8.7	0.61	-
941	292,010	0	-	-	-	-	-	68.0
945	292,900	0	2.67	-	4.93	8.3	0.60	-
950	294,000	0	2.69	-	5.21	8.0	0.72	68.8

ACKNOWLEDGMENTS

The authors thank Dr. J. Morley, Dr. W. Prell, Dr. A. Mix, Dr. D. Lazarus, Dr. W. Broecker, and Dr. G. Birchfield for useful suggestions. This represents a SPECMAP project contribution supported by the National Science Foundation Grant ATM80-19253.

REFERENCES

Berger, W. H. (1973). Deep-sea carbonates: Pleistocene dissolution cycles. *Journal of Foraminiferal Research* **3**, 187–195.

Birchfield, G. E., Weertman, J., and Lunde, A. T. (1981). A paleoclimate model of the Northern Hemisphere ice sheets. *Quaternary Research* **15**, 126–142.

Bloom, A. L., Broecker, W. S., Chappel, J. M. A., Matthews, R. K., and Mesolella, K. J. (1974). Quaternary sea level fluctuations on a tectonic coast: New $^{230}Th/^{234}U$ dates from the Huon Peninsula, New Guinea. *Quaternary Research* **4**, 185–205.

Broecker, W. S. (1966). Absolute dating and the astronomical theory of glaciation. *Science* **151**, 299–304.

Broecker, W. S. (1982). Ocean chemistry during glacial time. *Geochimica et Cosmochimica Acta* **46**, 1689–1705.

Broecker, W. S., Thurber, D. L., Goddard, J., Ku, T.-L., and Mesolella, K. J. (1968). Milankovitch hypothesis supported by precise dating of coral reefs and deep-sea sediments. *Science* **159**, 297–300.

Calder, N. (1974). Arithmetic of ice ages. *Nature (London)* **252**, 216–218.

Dodge, R. E., Fairbanks, R. G., Benninger, L. K., and Maurrasse, F. (1983). Pleistocene sea levels from raised coral reefs of Haiti. *Science* **219**, 1423–1425.

Dunn, D. A. (1982). Change from "Atlantic-type" to "Pacific-type" carbonate stratigraphy in the middle Pliocene Equatorial Pacific Ocean. *Marine Geology* **50**, 41–60.

Emiliani, C. (1966). Paleotemperature analysis of Caribbean cores P6304-8 and P6304-9 and a generalized temperature curve for the past 425,000 years. *Journal of Geology* **74**, 109–126.

Fairbanks, R. G., and Matthews, R. K. (1978). The marine oxygen isotope record in Pleistocene coral, Barbados, West Indies. *Quaternary Research* **10**, 181–196.

Hays, J. D., Imbrie, J., and Shackleton, N. J. (1976). Variations in the earth's orbit: Pacemaker of the ice ages. *Science* **194**, 1121–1132.

Imbrie, J., Hays, J. D., Martinson, D. G., McIntyre, A., Mix, A. C., Morley, J. J., Pisias, N. G., Prell, W. L., and Shackleton, N. J. (1984). The orbital theory of Pleistocene climate: Support from a revised chronology of the marine $\delta^{18}O$ record. *In* "Milankovitch and Climate, Part 1" (A. L. Berger *et al.*, Eds.), pp. 269–305. Reidel, The Netherlands.

Imbrie, J., and Imbrie, J. Z. (1980). Modelling the climatic response to orbital variations. *Science* **207**, 942–953.

Imbrie, J., and Kipp, N. G. (1971). A new micropaleontological method for quantitative paleoclimatology: Application to a late Pleistocene Caribbean core. *In* "The Late Cenozoic Glacial Ages" (K. K. Turekian, Ed.), pp. 71–181. Yale Univ. Press, New Haven, Conn.

Kominz, M. A., and Pisias, N. G. (1979). Pleistocene climate: Deterministic or stochastic. *Science* **204**, 171–173.

Martinson, D. G. (1982). "An Inverse Approach to Signal Correlation with Applications to Deep-Sea Stratigraphy and Chronostratigraphy." Ph.D. thesis, Lamont-Doherty Geological Observatory, Columbia University, New York.

Martinson, D. G., Menke, W., and Stoffa, A. (1982). An inverse approach to signal correlation. *Journal of Geophysical Research* **87**, 4807–4818.

Milankovitch, M. (1941). Kanon der Erdbestrahlung une sei Eiszeitenproblem. Acad. R. Serbe (Belegrade), ed. Spec. 133 Sect. Sci. Math. Naturales, 633, (translated by the Israel Program for Scientific Translations, Jerusalem, 1970).

Mix, A. C., and Ruddiman, W. F. (1986). Structure and timing of the last deglaciation: Oxygen-isotope evidence. *Quaternary Science Review*.

Moore, T. C., Jr., Pisias, N. G., and Dunn, D. A. (1982). Carbonate time series of the Quaternary and late Miocene sediments in the Pacific Ocean: A spectral comparison. *Marine Geology* **46**, 217–233.

Pisias, N. G., Martinson, D. G., Moore, T. C., Jr., Shackleton, N. J., Prell, W., Hays, J., and Boden, G. (1984). High resolution stratigraphic correlation of benthic oxygen isotopic records spanning the last 300,000 years. *Marine Geology* **56**, 119–136.

Ruddiman, W. F., and McIntyre, A. (1979). Warmth of the subpolar North Atlantic during Northern Hemisphere ice-sheet growth. *Science* **204**, 173–175.

Saltzman, B., Hansen, A. R., and Maasch, K. A., (1984). The late Quaternary glaciations as the response of a three-component feedback system to earth-orbital forcing. *Journal of the Atmospheric Sciences* **41**, 3380–3389.

Shackleton, N. J., (1977). Carbon-13 in Uvigerina: Tropical rainforest history and the Equatorial Pacific carbonate dissolution cycles. *In* "The Fate of Fossil Fuel CO_2 in the Oceans" (N. R. Anderson and A. Malahoff, Eds.), pp. 401–427. Plenum, New York.

Shackleton, N. J., and Opdyke, N. D. (1973). Oxygen isotope and paleomagnetic stratigraphy of Equatorial Pacific core V28-238: Oxygen isotope temperature and ice volumes on a 10,000 year and 100,000 year time scale. *Quaternary Research* **3**, 39–55.

Weertman, J. (1976). Milankovitch solar radiation variations and ice age ice sheet sizes. *Nature (London)* **261**, 17.